HHS Public Access

Author manuscript

*Stem Cells*. Author manuscript; available in PMC 2016 February 22.

Published in final edited form as:

*Stem Cells*. 2015 February ; 33(2): 557–573. doi:10.1002/stem.1868.

# Human Myocardial Pericytes: Multipotent Mesodermal Precursors Exhibiting Cardiac Specificity

**William C.W. Chen**[1,2,3,†,*], **James E. Baily**[5,6,7,*], **Mirko Corselli**[8,9], **Mary Diaz**[5,7], **Bin Sun**[3,4], **Guosheng Xiang**[2,3], **Gillian A. Gray**[5,7], **Johnny Huard**[2,3,4], and **Bruno Péault**[5,6,8,9,†]

[1]Department of Bioengineering, University of Pittsburgh, PA, USA 15260

[2]Department of Orthopedic Surgery, University of Pittsburgh, PA, USA 15260

[3]Stem Cell Research Center, University of Pittsburgh, PA, USA 15260

[4]McGowan Institute for Regenerative Medicine, University of Pittsburgh, PA, USA 15260

[5]Center for Cardiovascular Science, Queen's Medical Research Institute, University of Edinburgh, Scotland, UK EH16 4UU

[6]MRC Centre for Regenerative Medicine, University of Edinburgh, Scotland, UK EH16 4UU

[7]College of Medicine and Veterinary Medicine, University of Edinburgh, Scotland, UK EH16 4UU

[8]UCLA Orthopaedic Hospital, Department of Orthopaedic Surgery, University of California at Los Angeles, CA, USA 90095

[9]David Geffen School of Medicine, University of California at Los Angeles, CA, USA 90095

## Abstract

Perivascular mesenchymal precursor cells (i.e. pericytes) reside in skeletal muscle where they contribute to myofiber regeneration; however, the existence of similar microvessel-associated regenerative precursor cells in cardiac muscle has not yet been documented. We tested whether microvascular pericytes within human myocardium exhibit phenotypes and multipotency similar to their anatomically and developmentally distinct counterparts. Fetal and adult human heart

[†]Corresponding Authors: Bruno Péault, PhD, The BHF Regenerative Medicine Laboratory, MRC Centre for Regenerative Medicine, Edinburgh Bioquarter, 5 Little France Drive, Edinburgh UK EH16 4UU, Telephone: +44 (0)131 651 9505, Fax: +44 (0)131 651 9501. David Geffen School of Medicine at UCLA, Orthopaedic Hospital Research Center, University of California at Los Angeles, 615 Charles E. Young Drive South, Los Angeles, CA 90095-7358 USA, Telephone: 310-794-1339, Fax: 310-825-5409, bpeault@mednet.ucla.edu. William C.W. Chen, MD, PhD, Stem Cell Research Center, Department of Bioengineering and Orthopedic Surgery, University of Pittsburgh and UPMC, 450 Technology Drive Rm 236, Pittsburgh, PA 15219 USA, Telephone: 412-648-2798, Fax: 412-648-4066, chc88@pitt.edu.

[*]These authors contributed equally to this work

**Disclosure of Potential Conflicts of Interest**

JH received remuneration from Cook MyoSite, Inc. for consulting services and for royalties received from technology licensing during the period that the above research was performed. All other authors have no conflict of interest to disclose.

Authorship Contributions:

W.C.W.C. conception and design, collection and assembly of data, data analysis and interpretation, manuscript writing, and final approval of manuscript. J.E.B design, collection and assembly of data, data analysis and interpretation, and manuscript writing. M.C. collection of data, data analysis and interpretation. M.D. collection of data, data analysis and interpretation. B.S. collection of data, data analysis and interpretation. G.X. collection of data, data analysis and interpretation. G.G. design, administrative support, provision of study material or patients. J.H. design, financial support, provision of study material or patients. B.P. conception and design, data interpretation, financial support, final approval of manuscript.

pericytes (hHPs) express canonical pericyte markers *in situ*, including CD146, NG2, PDGFRβ, PDGFRα, αSMA, and SM-MHC, but not CD117, CD133 and desmin, nor endothelial cell (EC) markers. hHPs were prospectively purified to homogeneity from ventricular myocardium by flow cytometry, based on a combination of positive- (CD146) and negative-selection (CD34, CD45, CD56, and CD117) cell lineage markers. Purified hHPs expanded *in vitro* were phenotypically similar to human skeletal muscle-derived pericytes (hSkMPs). hHPs express MSC markers *in situ* and exhibited osteo- chondro-, and adipogenic potentials but, importantly, no ability for skeletal myogenesis, diverging from pericytes of all other origins. hHPs supported network formation with/without ECs in Matrigel cultures; hHPs further stimulated angiogenic responses under hypoxia, markedly different from hSkMPs. The cardiomyogenic potential of hHPs was examined following 5-azacytidine treatment and neonatal cardiomyocyte co-culture *in vitro,* and intramyocardial transplantation *in vivo*. Results indicated cardiomyocytic differentiation in a small fraction of hHPs. In conclusion, human myocardial pericytes share certain phenotypic and developmental similarities with their skeletal muscle homologs, yet exhibit different antigenic, myogenic, and angiogenic properties. This is the first example of an anatomical restriction in the developmental potential of pericytes as native mesenchymal stem cells.

### Keywords

pericyte; myocardium; tissue specificity; coronary vessel; stem cell; mesenchymal stem cell

## Introduction

The human heart has long been considered a terminally differentiated organ with no regenerative capacity (1). Recent discoveries of limited yet active turnover of human cardiomyocytes throughout adult life in addition to subsets of resident cardiac stem/progenitor cells raise the possibility that the human heart has an innate yet restricted regenerative potential (2–6). Other than the reported native cardiac precursor cells including Isl1+, c-kit+, Sca-1+ and cardiosphere-forming cells (7, 8), multipotent colony-forming precursor cells, similar to mesenchymal stem/stromal cells (MSCs), have been identified in the murine heart, occupying a perivascular adventitial niche (9). Lineage tracing in the embryo has revealed a proepicardial origin of these MSC-like cells. In addition, no interchange of this cell subset between bone marrow (BM) and local cardiac source after aging, myocardial injury, or even mobilization of BM stem cells in BM transplantation chimeras has been reported (9). Nevertheless, whether this MSC-like precursor cell population plays a critical role in cardiac development and regeneration remains to be investigated.

Microvascular mural cells, i.e. pericytes, tightly surround capillaries and microvessels (arterioles and venules) and play significant roles in vascular development, physiology and structural integrity (10, 11). The essential function of pericytes to recruit and stabilize endothelial cells (ECs) is critical to the success of angiogenesis during vascular maturation and remodeling (10, 11). We and others have shown that pericytes purified from a number of human organs, such as skeletal muscle, adipose, pancreas, placenta, umbilical cord, liver and retina, possess multi-lineage differentiation potential and stem/progenitor cell features

(12–18). Pericytes not only efficiently regenerate injured and dystrophic skeletal muscles but also effectively repair acutely infarcted hearts in mouse models, showing great promise in regenerative medicine (12–14, 19–21). Moreover, several populations of tissue-specific precursor cells have also been associated with the perivascular niche, suggesting a general supportive role for perivascular cells in tissue turnover and regeneration (22–24). Nevertheless, it remains to be tested whether native human cardiac pericytes exhibit the same cellular phenotypes and multipotency as their counterparts in other tissues. Furthermore, their potential developmental relationship with the aforementioned cardiac stem/progenitor cells awaits exploration.

Another important question yet to be answered is whether all pericytes are functionally equal. Pericyte populations appear to be variable physiologically among different organs and tissues, possibly reflecting their roles in regulating hydrostatic pressures and vascular homeostasis (25). Moreover, cardiac colony-forming precursors display unique lineage signatures distinct from those of their BM and aortic counterparts (9). This suggests that these MSC-like precursors arise from different developmental sources. More recently, depletion of coronary pericytes has been shown to be the underlying cause of sunitinib (an anti-cancer drug) induced cardiotoxicity in mice (26). Specifically, sunitinib was observed to be toxic to cardiac- but not skeletal muscle pericytes, further indicating a pathophysiological role unique to cardiac pericytes. Due to the difficulty of purifying multiple human pericyte populations from different organs simultaneously, it remains unclear if any tissue specificity exists among pericytes in terms of differentiation capacities and/or cellular behaviors in response to pathological conditions.

In this study, we report the molecular identification, prospective purification, long-term culture, and characterization of resident human heart pericytes (hHPs). The phenotypes and multipotency of purified hHPs were examined *in vitro* and *in vivo*. By comparing hHPs with human skeletal muscle pericytes (hSkMPs) isolated from the same donor, we investigated the tissue specificity and differential cellular responses to hypoxic conditions among pericytes of developmentally and functionally distinct tissue origins.

## Materials and Methods

### Human tissues

In total, 4 adult and 16 fetal independent human heart specimens were used for immunohistochemistry and cell isolation. Adult human cardiac biopsies were obtained postmortem from subjects that had died from non-cardiac causes. Adult human adipose tissue specimens were obtained anonymously from female patients undergoing abdominoplasty. The usage of adult human cardiac and adipose tissues was approved by Tayside Committee on Medical Research Ethics, NHS Scotland. Fetal human cardiac and skeletal muscle tissues (17 to 23 weeks of development) were obtained following voluntary or therapeutic pregnancy interruptions performed at Magee Womens Hospital of UPMC in Pittsburgh, PA, USA (in compliance with IRB protocol 0506176) as well as the Royal Infirmary in Edinburgh, Scotland, UK (in compliance with the University of Edinburgh Preclinical Ethics Committee and the UK Home Office PPL 60/4247). Developmental age

was estimated by measurement of foot length and medical history. Informed consent for the use of human fetal tissues was obtained from patients in all instances.

## Cell isolation

Fresh adult and fetal human cardiac tissues were processed for cell isolation. Briefly, atria, heart valves, and major blood vessels were grossly removed, followed by microscopic removal of pericardium and endocardium from the ventricles. Ventricular myocardium was first cut into small pieces in Dulbecco's modified Eagle medium (DMEM, Invitrogen, Life Technologies) containing 10% fetal bovine serum (FBS, Invitrogen), 1% penicillin-streptomycin (P/S, Invitrogen), mechanically minced, and subsequently digested with a mixture of collagenases I, II and IV (1 mg/mL, Sigma-Aldrich) for 15–20 minutes (depending on the specimen size) under agitation at 37°C. After centrifugation, pellets were washed and resuspended in erythrocyte lysis buffer (155 mM $NH_4Cl$, 10mM $KHCO_3$, 0,1mM EDTA) and incubated for 10 min at room temperature. Cells were then washed and sequentially filtered through 100- and 70-μm cell strainers (BD Falcon) to obtain single cell suspensions. Fresh fetal human skeletal muscle specimens were obtained from the same donor and processed for cell isolation according to the previously published protocol (13).

## Fluorescence-activated cell sorting (FACS) and flow cytometry analysis

For cell sorting, cells ($2–5\times10^6$) in suspension were incubated with all of the following fluorochrome-conjugated mouse anti-human antibodies (all with 1:100 dilutions): anti-CD34-APC (Becton-Dickinson), anti-CD45-APC-Cy7 (Santa Cruz Biotechnology), anti-CD56-PE-Cy7, anti-CD117-PE, and anti-CD146-FITC (all from AbD Serotec) in DMEM supplemented with 5% FBS and 1% P/S at 4°C for 20 min in the dark. As negative controls, cells were labelled with isotype-matched mouse IgGs conjugated with APC, PE-Cy7 (both from Becton-Dickinson), APC-Cy7 (Santa Cruz Biotechnology), PE and FITC (both from Chemicon, Millipore). After washing and immediately prior to cell sorting, all labelled cells were incubated with 7-amino-actinomycin D (7-AAD) (Becton-Dickinson, 1:100) or 4′,6-diamino-2-phenylindole dihydrochloride (DAPI) (Sigma Aldrich, 1:400) for dead cell exclusion and then run on a FACSAria flow cytometer (Becton-Dickinson). We first gated out the CD117+ population before selecting the CD45−/CD56− population for subsequent gating on CD34 and CD146. Purified hHPs (CD146+/CD34−/CD45−/CD56−/CD117−) were collected and cultured over the long term. Human skeletal muscle-derived pericytes (hSkMPs) and fat-derived pericytes were sorted according to our previously published protocol (13).

Flow cytometry was employed to examine the expression profile of cell lineage markers. Briefly, freshly sorted hHPs or cultured hHPs at different passages were labelled with the following fluorochrome-conjugated antibodies (all with 1:100 dilutions): anti-CD34-APC, anti-CD44-PE, anti-CD90-APC, anti-CD146-PE, anti-platelet-derived growth factor receptor-β (PDGFRβ)-PE (all from Becton-Dickinson), anti-CD73-PE, anti-CD105-PE (both from Invitrogen, Life Technologies), anti-CD45-APC-Cy7 (Santa Cruz Biotechnology), anti-CD56-PE-Cy7, anti-CD117-PE, and anti-CD146-FITC (all from AbD Serotec), for 20 min at 4°C in the dark and subsequently analyzed on a FACSAria flow cytometer.

### Cell culture and cell labelling

Freshly sorted hHPs were initially seeded at $2\times10^4$ cells/cm$^2$ in complete endothelial cell growth medium-2 (EGM-2, Lonza) and cultured at 37°C for 2 weeks on plates coated with 0.2% gelatin (Calbiochem) until confluence. hHPs were then detached by 0.25% trypsin-EDTA (Invitrogen, Life Technologies) treatment for 10 min at 37°C, split at a 1:3 ratio, and seeded on uncoated plates with pericyte maintenance medium: DMEM high glucose (Invitrogen, Life Technologies) supplemented with 20% FBS and 1% P/S. After the third passage, cells were passaged at a 1:5–1:6 ratio and maintained in the same conditions with culture medium changed every 3–4 days. The population doubling time (PDT) was calculated as previously described (13). Sorted hSkMPs were expanded and maintained in the same conditions as hHPs. Single donor-derived human umbilical cord vein endothelial cells (HUVECs) were purchased from Lonza and cultured in EGM-2 medium, following the manufacturer's instructions.

For the gene transfer of green fluorescence protein (GFP), cultured hHPs at passages 4–6 were detached with 0.25% trypsin-EDTA and seeded at a density of 10,000 cells/cm$^2$. After 24–48 hours, when the hHP culture reached around 70% confluence, the medium was replaced with the transduction medium (α-MEM with 10% FBS, 1% P/S and 8 μg/mL polybrene) containing a lentivirus-based CMV-driven eGFP expression vector at MOI of 10. Following incubation for 16–18 hours at 37°C, the transduction medium was removed and replenished by pericyte maintenance medium. Three days later, nearly 95% of cells expressed GFP. GFP+ cells were further expanded in pericyte maintenance medium for 1–2 passages with no apparent adverse effect. For short-term *in vitro* experiments, cells were labelled with cell membrane fluorescent dyes, PKH26 (red) and PKH67 (green) (both from Sigma-Aldrich), following the manufacturer's instructions. Dye-labeled cells were used in experiments immediately after labelling without further expansion.

### Immunohistochemical and immunocytochemical analyses

Human heart specimens were preserved at −80°C and cryosectioned at 8–10 μm thickness. Sections were fixed in a pre-cooled (−20°C) mixture of methanol (Fisher Scientific) and acetone (VWR International) (1:1) for 5 min or in pre-cooled acetone for 5 min (for human spectrin) prior to staining. For immunocytochemistry, cultured hHPs were washed twice with PBS and fixed in pre-cooled methanol for 5 min. Non-specific antibody binding was blocked with 5% donkey or goat serum in PBS for 1 hour at room temperature and, if necessary, with the Mouse-on-Mouse (M.O.M.) antibody staining kit (Vector Laboratories). The following uncoupled primary antibodies were used (diluted with 5% donkey or goat serum in PBS): mouse anti-human-CD31 (Santa Cruz Biotechnology), -CD144 (Beckman Coulter), -NG2 (chondroitin sulphate), -CD34, -CD146 (all from Becton-Dickinson), -Nkx2.5, -PDGFRβ (both from R&D Systems), -α-sarcomeric actinin (Sigma-Aldrich), -cardiac myosin heavy chain (Chemicon, Millipore), -GATA4, rabbit anti-human-PDGFRα (both from Santa Cruz Biotechnology), rabbit anti-human-CD117 (c-kit) (Abcam), and goat anti-vimentin (Sigma-Aldrich) (all at 1:100 dilutions); mouse anti-human-CD44, -CD90 (both from Becton-Dickinson), -CD73, -CD105 (both from Invitrogen, Life Technologies), -smooth muscle myosin heavy chain (DAKO), and sheep anti-human-alkaline phosphatase (AbD Serotec) (all at 1:50 dilutions) at 4°C overnight. The following conjugated primary

antibodies were used: anti-mammalian alpha-smooth muscle actin (αSMA)-FITC (Sigma-Aldrich) and -von Willebrand factor (vWF) (US Biological), biotinylated anti-human CD144 (Becton-Dickinson) (all at 1:100 dilutions), and biotinylated anti-human CD146 (Miltenyi Biotec, 1:20). Skeletal muscle proteins were detected with mouse anti-fast skeletal myosin heavy chain, anti-slow skeletal myosin heavy chain, anti-desmin (all from Sigma-Aldrich), and anti-spectrin (Novocastra, Leica Biosystems) (all at 1:100 dilutions). Directly biotinylated *Ulex europaeus* lectin (UEA-1) was used as an endothelial cell marker for long-term cultured cells (Vector Laboratories, 1:200).

After rinsing with PBS three times, sections or cells were incubated for 1 hour at room temperature with a fluorochrome-conjugated secondary antibody at 1:300 dilutions, including anti-mouse-Alexa488 IgG, anti-mouse-Alexa555 IgG (both from Molecular Probes, Life Technologies), anti-mouse-Cy3 IgG, anti-rabbit-Alexa488 IgG, anti-rabbit-Cy3 IgG, anti-sheep-Alexa488 IgG (all from Jackson ImmunoResearch Laboratories); or with biotinylated secondary antibody and then with fluorochrome-coupled streptavidin (both at 1:500 dilutions), including goat anti-mouse biotinylated IgG antibodies (DAKO and Immunotech), streptavidin-Cy3 (Sigma-Aldrich), and streptavidin-Cy5 (Molecular Probes, Life Technologies); all diluted in 5% donkey or goat serum in PBS. Nuclei were stained with DAPI (Molecular Probes, 1:2000) for 5 min at room temperature. An isotype-matched negative control was performed with each immunostaining. Slides were mounted in glycerol-PBS (1:1, Sigma-Aldrich) and observed on an epifluorescence microscope (Nikon Eclipse TE 2000-U). Alternatively, sections were analyzed and photographed on an Olympus Fluoview 1000 confocal microscope (equipped with 20x-100x oil immersion optics) at the Center for Biologic Imaging, University of Pittsburgh.

### Matrigel culture/co-culture in vitro

Cell culture and co-culture experiments using 2D and 3D Matrigel systems were performed; capillary-like network formation was recorded. In brief, 350μl of Matrigel (Becton-Dickinson) was placed in each well of a 24-well plate and incubated at 37°C for 30 min. Fifty thousand hHPs were trypsinized, washed, and re-suspended in 700μl of EGM2 and subsequently seeded onto a Matrigel-coated well. Experiments using $5\times10^4$ HUVECs or $5\times10^4$ isogeneic hSkMPs were performed as controls. A 2D co-culture system using cells pre-labeled with PKH26 and PKH67 cell membrane dyes was used to observe hHP-HUVEC interactions. Briefly, $5\times10^4$ PKH26-labeled HUVECs (red) and $5\times10^4$ PKH67-labeled hHPs (green) were well mixed, re-suspended in 700μl of EGM2, seeded onto Matrigel in a 24-well plate, and further co-cultured for 24 hours. An *in vitro* 3D Matrigel culture/co-culture system was developed to investigate the vascular supportive function of hHPs. In short, $25\times10^4$ PKH67-labeled hHPs (green) were re-suspended in EGM2 and well mixed with 350μl of Matrigel at a 3:1 ratio before being encapsulated into one well of a 24-well plate and subsequently incubated for 72 hours. A small amount of EGM2 was added on top of the plugs after gelation and exchanged every 24–48 hours. Experiments using $25\times10^4$ PKH26-labeled HUVECs were performed as controls. A 3D co-culture system using $25\times10^4$ PKH26-labeled HUVECs (red) and $25\times10^4$ PKH67-labeled hHPs (green) was conducted in the same manner and subsequently incubated for 72 hours under 21% $O_2$. Another set of Matrigel co-culture plugs were simultaneously exposed to hypoxic environment for 72 hours

(described in Hypoxia assay). The same 3D Matrigel co-culture experiments using PKH26-labeled HUVECs (red) and PKH67-labeled isogeneic hSkMPs (green) were performed for comparison. All experiments were independently repeated 3 times. Images were taken using an epi-fluorescence microscope (Nikon Eclipse TE 2000-U). Alternatively, 2D Matrigel culture and 3D Matrigel culture/co-culture plugs were analyzed and photographed on an inverted confocal microscope (Olympus Fluoview 1000) at the Center for Biologic Imaging, University of Pittsburgh. Three-dimensional image reconstruction was accomplished by the Olympus Fluoview software using multiple 2D slices taken serially along the vertical axis. Capillary-like cord length in 3D Matrigel co-culture plugs (N=3 plugs per group) was quantified by 4 random measurements of cord length taken from each image with 3 images per plug at each time point. Results were averaged.

### Hypoxia assay

To assess the influence of hypoxic environment on the angiogenic response of isogeneic hHPs and hSkMPs, we cultured 3D Matrigel co-culture plugs under 2.5% $O_2$ concentration (with 5% $CO_2$ and 92.5% $N_2$) *in vitro* as formerly described (21). Concisely, 3D Matrigel plugs containing evenly mixed PKH26-labeled HUVECs and either PKH67-labeled hHPs or isogeneic PKH67-labeled hSkMPs were fabricated as mentioned above under ambient oxygen concentration (21% $O_2$). Plugs were immediately exposed to 2.5% $O_2$ before gelation of the plugs and subsequently incubated for 72 hours. Plugs were removed from hypoxia for 10–15 min every 24 hours for imaging under room air. The same Matrigel co-culture plugs simultaneously exposed to 21% $O_2$ served as controls.

### RT-PCR and Semi-quantitative RT-PCR

Total RNA was extracted from $10^4$ cells using the Absolutely RNA nanoprep kit (Stratagene). cDNA was synthesized with SuperScript™ II reverse transcriptase (Invitrogen, Life Technologies). PCR was performed for 30 cycles at 58°C annealing temperature with Taq polymerase (Invitrogen, Life Technologies). PCR products were electrophoresed on 1% agarose gels. The primers used for PCR are listed in Supplemental Table 1. Each set of oligonucleotides was designed to span two different exons to avoid issues relating to genomic DNA contamination.

For semi-quantitative RT-PCR, total RNA was extracted from cells using RNeasy Mini Kit 50 (Qiagen Sciences) and treated with an RNase-free DNase set (Qiagen Sciences). RNA concentration and quality (A260/280) were assessed using NanoDrop 1000 Spectrophotometer (Thermo Scientific). RNA integrity was assessed through 1% agarose gel electrophoresis. From each sample, 500ng of total RNA were reverse transcribed with SuperScript III Reverse Transcriptase (Life Technologies). Analysis of transcripts was performed with primer pairs specifically designed for human cardiomyogenic genes using USCS Genome Browser (Supplemental Table 2). A master mix of the following components was prepared in nuclease free water (Qiagen Sciences): 1X MyTaq Reaction Buffer (Bioline Ltd), 0.1 mM (each) dNTPs (Bioline Ltd), 0.25 μM (each) primers and 1U MyTaq DNA Polymerase (Bioline Ltd). Nineteen microliters of master mix were added to 1 μl cDNA, and PCR reactions were carried out in a Veriti 96-Well Thermal Cycler (Applied Biosystems, Life Technologies) using the following program: single denaturation at 95°C for 3 minutes,

35 cycles of amplification at (95°C for 15 seconds, 55°C for 15 seconds and 72°C for 10 seconds), and final extension at 72°C for 5 minutes. The PCR products were verified by 2% agarose gel electrophoresis. Images were captured using the Alpha DigiDoc 1201 software (Genetic Technologies)

### Multi-lineage differentiation in culture

**Osteogenesis—**For *in vitro* bone formation, cells at 70% confluence were cultivated in DMEM supplemented with 10% FBS, 0.1 μM dexamethasone, 50 μg/ml L-ascorbic acid, and 10 mM beta-glycerophosphate (13). Three weeks later, cells were fixed in 4% formaldehyde for 2 min and incubated for 10 min with alizarin red, pH 4.2 for the detection of calcium deposits (all reagents from Sigma-Aldrich).

**Chondrogenesis—**Pellet culture was performed by spinning down $3\times10^5$ cultured cells in each 15ml conical tube (BD Falcon) which were then grown in serum-free DMEM containing an insulin-transferrin-selenious acid mix (ITS) (Becton-Dickinson), 50 μg/ml L-ascorbic acid 2-phosphate (WAKO), 100 μg/ml sodium pyruvate, 40 μg/ml L-proline (both from Invitrogen, Life Technologies), 0.1 μM dexamethasone (Sigma-Aldrich) and 10 ng/ml transforming growth factor β1 (TGF-β1; Peprotech) (13). Three weeks later, pellets were fixed in 10% formalin, dehydrated in ethanol, and embedded in paraffin. Sections (5 μm thick) were rehydrated and stained with Alcian blue and nuclear fast red for the detection of sulfated glycosaminoglycans and nuclei, respectively.

**Adipogenesis—**Cultured cells at 70% confluence were switched to adipogenic medium: DMEM containing 10% FBS, 1 μM dexamethasone, 0.5 μM isobutylmethylxanthine, 60 μM indomethacine, and 170 μM insulin (all from Sigma-Aldrich) (13). Two weeks later, cells were fixed in 2% paraformaldehyde (PFA) at room temperature, washed in 60% isopropanol, and incubated with Oil red O for 10 min at room temperature for the detection of lipids.

**Skeletal myogenesis—**Cells ($2\times10^3$ cells/$cm^2$) were cultured for 7 days in muscle proliferation medium: DMEM high-glucose supplemented with 10% FBS, 10% horse serum (HS, Invitrogen), 1% chicken embryo extract (CEE; Accurate Chemical), and 1% P/S, and subsequently for additional 7 to 10 days in myogenic (muscle fusion) medium: DMEM high-glucose supplemented with 1% FBS, 1% HS, 0.5% CEE, and 1% P/S. Half of the medium was renewed every 3 days (13). Skeletal myogenesis was induced by lowering total serum concentration from 20% to 2% until elongated, multinucleated skeletal myofibers appeared.

**Cardiomyogenesis—**Cells ($2\times10^3$ cells/$cm^2$) were seeded and cultured for 1–2 days in pericyte maintenance medium. The medium was then replaced with cardiomyogenic induction medium: DMEM high-glucose supplemented with 10% FBS, 10 μg/l basic fibroblast growth factor (bFGF), 10 μM 5-azacytidine, and 1% P/S for 72 hours (9). After washing, cells were cultured in pericyte maintenance medium for additional 14 days.

### Skeletal myogenesis in vivo

To examine skeletal myogenesis of hHPs *in vivo*, we performed cell transplantation in an immunodeficient mouse model of muscle injury. The Institutional Animal Care and Use Committee at Children's Hospital of Pittsburgh of UPMC and University of Pittsburgh approved the animal usage and surgical procedures performed in this study (Protocols #15-04 and #0810310). A total of 8 female non-obese diabetic/severe combined immunodeficiency (NOD/SCID) mice (6 weeks old) (Jackson Laboratory, Bar Harbor, ME, USA) were used for this study. Briefly, NOD/SCID mice were anaesthetized by inhalation of isoflurane/$O_2$ mixture. Cardiotoxin (CTX, 15μg; Accurate Chemical), diluted in 20μL PBS, was injected into the gastrocnemius muscle three hours prior to cell transplantation. Mice were then re-anaesthetized, and $5.0\times10^4$ cells suspended in 30μL PBS were slowly injected into the injured muscle. Controls were injected with the same volume of PBS after the induction of muscle injury. Mice were sacrificed 2 weeks later. Gastrocnemius muscles were dissected and flash frozen in 2-methylbutane (Sigma-Aldrich) pre-cooled in liquid nitrogen and subsequently embedded in tissue freezing medium (Triangle Biomedical Sciences). Samples were preserved at −80°C and cryosectioned at 8–10μm thickness for immunohistochemical analyses.

### Pericyte/cardiomyocyte co-culture in vitro

Rat neonatal cardiomyocytes were isolated from anaesthetized 3-day-old rat pups using the Worthington rat neonatal cardiomyocyte isolation system per the manufacturer's protocol (Worthington Biochemical Corp). Pericyte/cardiomyocyte co-culture protocol was adopted and modified from previous reports (27, 28). Briefly, cells were resuspended in induction medium containing Dulbecco's Modified Eagle Medium – GlutaMax and Medium M199 (4:1) supplemented with 10% HS, 5% FBS and 1% P/S and seeded on 1% gelatin coated plates (some containing glass coverslips) at a density of 4,000 cells/$cm^2$. After 72 hours, induction medium was exchanged for fresh maintenance medium containing DMEM/M199 (4:1), 10% FBS and 1% P/S supplemented with 3 μg/ml of Mitomycin C (Sigma-Aldrich) and incubated for 2 hours. Rat neonatal cardiomyocytes were then washed with PBS before labeled pericytes at a density of 1,000 cells/$cm^2$ resuspended in un-supplemented maintenance medium were added. Labeling of pericytes was achieved with either CM-Dil CellTracker (Invitrogen), according to the manufacturer's instructions, or GFP lentiviral transduction as previously described (21). Alternatively, labelled pericytes were first treated with 5 μM of 5-azacytidine for 3 days as formerly described before being seeded with rat cardiomyocytes (28). At 10, 14, and 21 days, co-cultures were examined under phase contrast and fluorescence channels; time-lapse image series were acquired using an inverted fluorescence microscope (Zeiss Observer) and AxioVision LE software (Zeiss). For immunocytochemistry, coverslips were removed and fixed with 4% PFA for 10 minutes at room temperature and then washed twice with PBS before being stained for α-Actinin (Sigma Aldrich, 1:800) and cardiac-specific troponin-T (Abcam, 1:200) and examined using an upright fluorescence microscope (Olympus Bx61) and Volocity 3D Image Analysis Software (Perkin Elmer). Cells in wells without coverslips were preserved with TRIzol reagent (Life technologies). Controls were performed using labeled pericytes cultured in parallel in cardiomyocyte induction then maintenance media for 21 days. Pericyte/

cardiomyocyte co-cultures were independently repeated multiple times with three populations of hHPs between passages 4 and 5 as well as a single population of human adult fat pericytes at passage 4. Human fat pericytes were used as a control pericyte population due to the unavailability of matching hSkMPs at the time of this particular set of experiments.

### Detection of calcium flux in vitro

Cells in above cardiomyogenic co-culture wells were separately loaded with the acetoxymethyl ester form of fluo-4 (5 μmol/L, Life Technologies) for 30 minutes at room temperature (23°C). A modified tyrode solution was added to excess, to stop the loading process (29). The cells were then left to de-esterify in an incubator at 37°C for 30 minutes. Each well was examined using an Olympus IX51 fluorescence microscope and images acquired using Volocity imaging software (Perkin Elmer). hHPs were identified by the presence of CM-Dil dye emitting at 570nm (red channel) whilst calcium bound Fluo-4 fluorescence was detected at 506nm and recorded (green channel).

### Cardiac myogenesis in vivo

To evaluate the cardiomyogenic potential of hHPs *in vivo*, cell transplantation was performed in acutely infarcted and healthy immunodeficient mouse hearts. The Institutional Animal Care and Use Committee at Children's Hospital of Pittsburgh (Protocols #55-07), University of Pittsburgh (Protocols #0901681A-5), and University of Edinburgh approved the animal usage and surgical procedures. A total of 9 male NOD/SCID mice (12 weeks old) (Jackson Laboratory, Bar Harbor, ME, USA) were used. For the ischemic injury model, myocardial infarction (MI) was induced by ligation of the left anterior descending coronary artery. Intramyocardial injections of transduced GFP+ hHPs ($3\times10^5$ cells per heart) were performed at 3 sites 5 minutes after the induction of MI as previously described (21). Alternatively, $3\times10^5$ cells GFP+ hHPs were intramyocardially injected into normal NOD/SCID hearts with no ischemic injury. At 1 and 3 week post-surgery, hearts were harvested and processed as previously described (21). Heart specimens were cryosectioned at 6–8μm thickness and used for immunohistochemical analyses. The presence of GFP+ hHPs was detected by immunofluorescent or immunohistochemical staining using rabbit anti-GFP antibody (Abcam, 1:1000) or goat anti-GFP antibody (Abcam, 1:200) performed on 4% paraformaldehyde-fixed sections as previously reported (21). Co-stainings of anti-GFP with mouse anti-cardiac troponin-I (Abcam, 1:100) and/or rabbit anti-connexin 43 (Millipore, 1:200) were employed to detect co-expression of cardiac troponin-I and/or connexin 43 by transplanted GFP+ hHPs.

### Statistical analysis

All measured data are presented as mean ± standard deviation (SD). Statistical differences were analyzed by one-way ANOVA (multiple groups) with 95% confidence interval. Bonferroni test was performed for post-hoc multiple comparison analysis of one-way ANOVA. Statistical analyses were performed with SigmaStat statistics software.

## Results

### Identification of resident microvascular pericytes within the human ventricular myocardium

To investigate whether pericytes residing in human myocardium express previously reported pericyte markers, two adult and five fetal ventricular biopsies were examined. We observed consistent expression of pericyte markers by human myocardial perivascular cells surrounding microvessels (diameter 10–100 μm) and capillaries (diameter less than 10 μm), including NG2 (Fig. 1A) and CD146 (Fig. 1A–C and G–I), α-smooth muscle actin (αSMA) (Fig. 1B), smooth muscle myosin heavy chain (SM-MHC) (Fig. 1C), PDGFRβ (Fig. 1D) and PDGFRα (Fig. 1E), but not desmin (Fig. 1F). Co-expression of NG2 and CD146 (Fig. 1A, main and inset), CD146 and αSMA (Fig. 1B, main and inset) as well as CD146 and SM-MHC (Fig. 1C) by ventricular pericytes was detected at microvessels of different sizes. PDGFRβ was detected on all myocardial pericytes (Fig. 1D, red arrows). The expression of PDGFRα, a multipotent cardiovascular precursor cell marker, was found on nearly all pericytes surrounding microvessels but only on some around capillaries (Fig. 1E, red arrows). Consistent with our previous reports, endothelial cell (EC) markers, including CD34 (Fig. 1G), von Willebrand factor (vWF) (Fig. 1D–F and H), CD144 (VE-cadherin) (Fig. 1H, inset), and CD31 (Fig. 1I), were not expressed by myocardial pericytes. Unlike peri-capillary pericytes in other human tissues which may express αSMA (13), expression of αSMA (Fig. 1B, main and inset) and SM-MHC (Fig. 1C) were only noted in cells surrounding arterioles and venules but not around capillaries. Desmin, a validated pericyte marker in many human organs (30, 31), was not expressed by microvascular pericytes in ventricular myocardium (Fig. 1F, main and inset). In addition, myocardial pericytes (Supplemental Fig. 1A–C, purple arrows) did not express CD117 (c-kit, a cardiac progenitor marker) while approximately one third of CD117+ cells (Supplemental Fig. 1A–D, red arrows) within the ventricular myocardium were juxtaposed to CD146+ pericytes and/or vWF+ ECs (Supplemental Fig. 1A–D, green arrows) in microvessels/capillaries. Although some epicardial/pericardial cells expressing Wilm's Tumor 1 (Wt1, an epicardial progenitor marker), were located adjacent to vWF+ blood vessels, no myocardial perivascular cells displaying Wt1 was identified (Supplemental Fig. 2A–B). Negative controls for immunohistochemistry were shown in Supplemental Fig. 3. We did not notice qualitatively appreciable difference in antigen distribution patterns between examined adult and fetal myocardial tissues. These results indicate that myocardial pericytes natively display a similar profile of cell surface markers as those found in other human organs and yet manifest cardiac specificity antigenically.

### Purification and culture of human heart pericytes

To prospectively purify human myocardial pericytes using multi-color fluorescence-activated cell sorting (FACS), two adult and 12 fetal (17 to 23 weeks) heart samples were independently processed. Briefly, the epicardium and endocardium were microscopically removed; only ventricular myocardium was collected for mechanical dissociation and collagenase digestion. Before being subjected to FACS purification, cells were stained with fluorescence-conjugated antibodies against a panel of selective cell lineage markers, including CD34 (endothelial cells), CD45 (hematopoietic cells), CD56 (neural/

myogenic/NK cells), CD117 (hematopoietic/cardiac precursor cells), and CD146 (pericytes/endothelial cells). To be devoid of contamination from circulating hematopoietic and/or resident cardiac precursor cells, CD117+ cells were initially gated out of myocardial cell suspensions, followed by the exclusion of CD45+ and CD56+ cells as described in our previously published protocols (Fig. 2A) (13). Human heart pericytes (hHPs) were subsequently identified by robust CD146 expression and absence of CD34 to avoid EC contamination (Fig. 2A). hHPs (CD146+/CD34−/CD45−/CD56−/CD117−) were sorted to homogeneity at an average frequency of 1.21±0.52%, in the same range as the reported ratio of pericytes (CD146+/CD34−/CD45−/CD56−) in other human organs (13, 14).

Sorted hHPs were cultured in pericyte maintenance medium and commonly exhibiting an elongated, rectangular morphology with extended arms, similar to their skeletal muscle counterparts at sub-confluence (Fig. 2B). RT-PCR analysis confirmed the homogeneity of freshly sorted hHPs with no contamination by ECs (Fig. 2C). Purified hHPs did not express CD117 and can be cultured over the long term while maintaining expression of the same selection marker profile (Supplemental Fig. 4A). The growth of hHPs in long-term culture was comparable to that of human skeletal muscle pericytes (hSkMPs) (13): a population doubling time (PDT) of approximately 65 hours between passages 3–12 (Supplemental Fig. 4B), with occasional formation of spherical structures at early passages (Supplemental Fig. 4C); no apparent contact inhibition at confluence; and maximal population doublings of forty or more; except for a seemingly shorter initial growth retardation (first 4 weeks after sorting) (Supplemental Fig. 4B). Immunocytochemistry revealed that cultured hHPs express common pericyte markers including CD146 (Fig. 2D, a), alkaline phosphatase (ALP) (Fig. 2D, b), αSMA (Fig. 2D, c), NG2 (Fig. 2D, d), PDGFRβ (Fig. 2D, e), and vimentin (Supplemental Fig. 4D, a) but no desmin (Supplemental Fig. 4D, b), CD3 (Supplemental Fig. 4D, c), or CD19 (Supplemental Fig. 4D, d). hHPs also notably express PDGFRα (Fig. 2D, f), a multipotent cardiovascular precursor cell marker. Further analyses of cultured hHPs using flow cytometry not only confirmed the exhibition of positive selection markers such as CD146, ALP, PDGFRβ, and PDGFRα (Supplemental Fig. 4E), but also showed the expression of classic MSC markers, including CD44, CD73, CD90 and CD105, similar to pericytes purified from other tissue origins (Supplemental Fig. 4E). Negative controls for immunocytochemistry were shown in Supplemental Fig. 5.

### Human heart pericytes natively express MSC markers

As we and others have previously shown that microvascular pericytes in many tissues manifest canonical MSC markers *in situ*, we investigated whether hHPs indigenously exhibit this MSC phenotype in the myocardium. Immunohistochemistry revealed that hHPs surrounding ECs of small blood vessels in the ventricular myocardium natively express classic MSC markers, including CD44 (Fig. 3A), CD73 (Fig. 3B), CD90 (Fig. 3C, main and inset), and CD105 (Fig. 3D). Particularly, only microvascular pericytes expressed CD105 (Fig. 3D enlargement, red arrows), whereas perivascular cells surrounding larger blood vessels did not (Fig. 3D, dotted encirclement). Confocal microscopy confirmed the co-expression of CD146 and CD44 (Fig. 3E) or CD90 (Fig. 3F) by hHPs. Flow cytometry was further employed to validate that freshly purified hHPs retain the expression of MSC

markers. The results showed that hHPs (CD146+/CD34−/CD45−/CD56−/CD117−) (Fig. 3G, a) co-express ALP, CD44, CD73, CD90, and CD105, but not CD133 (Fig. 3G, b–g).

## Human heart pericytes exhibit mesodermal differentiation capacity but, distinctively, no skeletal myogenesis potential

After demonstrating that hHPs manifest MSC markers natively and in culture, we investigated whether hHPs possess multi-lineage differentiation potential, thus resembling pericytes originated from other organs. Cultured hHPs were incubated in inductive conditions for osteo-, chondro-, adipo-, and skeletal myogenesis respectively. Neither hHPs nor hSkMPs expressed typical skeletal myogenic genes in culture (Supplemental Fig. 6). Compared with hSkMPs, which exhibited all four mesodermal lineage differentiations (Fig. 4A, e–h), hHPs displayed robust osteo-, chondro-, and adipogenic differentiation but no skeletal myotube formation, even after extended incubation for up to 3 weeks (Fig. 4A, a–d). We further examined the difference between hHPs and hSkMPs in skeletal myogenesis *in vitro* using immunocytochemistry. Differentiated hSkMPs expressed both immature and mature skeletal muscle proteins, including desmin, fast skeletal myosin heavy chain (FS-MHC), and slow skeletal myosin heavy chain (SS-MHC) (Fig. 4B, a–c) while hHPs did not display any of the three muscle markers after culturing in myogenic medium for 7 days (Fig. 4B, d–f). To investigate whether this tissue-specific difference in skeletal myogenesis sustains *in vivo*, fifty thousand cultured hHPs or hSkMPs isolated from the same donor were injected into cardiotoxin-injured hind-limb skeletal muscles of immunodeficient mice (N=4 per group) for 2 weeks. Immunohistochemistry with human-specific anti-spectrin antibody showed that only hSkMPs regenerated human myofibers while no human spectrin-positive myofiber was detected in any hHP-injected muscles (Fig. 4C).

## Human heart pericytes support microvascular structures yet exhibit distinctive angiogenic behaviors in response to hypoxia

To test whether hHPs support the formation of microvascular structures, we utilized 2D and 3D Matrigel cultures/co-cultures as previously reported (21). hHPs alone seeded into Matrigel-coated wells formed network structures within 6–12 hours (Fig. 5A), resembling typical capillary-like networks formed by HUVECs during the same time frame (Fig. 5B). Confocal microscopy with 3D image reconstruction showed formation of tubal structures by dye-labeled hHPs (PKH67, green) in Matrigel-coated culture at 72 hours (Fig. 5C and Supplemental Video 1), comparable to endothelial tubes formed by dye-labeled HUVECs (PKH26, red) (Fig. 5D and Supplemental Video 2). When co-cultured, dye-labeled hHPs (green) and HUVECs (red) co-formed network structures within 6–12 hours (Fig. 5E), with HUVECs morphologically aligning with hHPs (Fig. 5F). To further mimic native capillary formation, 3D Matrigel plugs encapsulating evenly distributed hHPs or HUVECs were created *in vitro*. Dye-labeled hHPs (green) formed 3D network structures with structural maturation and/or remodeling over time (Fig. 5G–I) while HUVECs (red) did not form any organized structure under the same culture conditions (Fig. 5J–L). Three-dimensional reconstructed confocal animation further illustrated multiple tubal structures formed by hHPs (green) alone within a 3D Matrigel plug at 180 hours (Supplemental Video 3).

Three-dimensional Matrigel co-culture plugs were further used to study reciprocal influence between hHPs and ECs maintained under ambient (21%) or hypoxic (2.5%) oxygen concentration. To investigate whether pericytes isolated from different tissue origins hold similar microvascular supportive functionality, hHPs and hSkMPs purified from the same donor were compared. Co-cultured hHPs (green) and HUVECs (red) gradually migrated and formed 3D network structures inside Matrigel plugs within 72 hours under 21% $O_2$ (Fig. 5M, a–c). Confocal microscopy with z-stack image reconstruction further revealed organization of dual-layer tubal structures by hHPs (green) and HUVECs (red) in Matrigel plugs, with HUVECs forming a central endothelial tube whilst hHPs tightly surrounding the HUVEC tube (Supplemental Fig. 7 and Video 4). Such an angiogenic process appeared to be facilitated over time when hHP-HUVEC plugs were exposed to hypoxic conditions (Fig. 5M, d–f). On the other hand, hSkMPs co-formed network structures with HUVECs under 21% $O_2$, comparable to those formed in hHP-HUVEC plugs (Fig. 5M, g–i). However, when exposed to hypoxic conditions, hSkMP-HUVEC plugs showed markedly diminished sprouting and network formation (Fig. 5M, j–l). Quantification of capillary-like cord length revealed that hHP-HUVEC plugs under hypoxic conditions exhibit the most extensive network formation among all groups ($p<0.001$ at 24 and 48 hrs; $p \leq 0.005$ at 72 hrs) while hSkMP-HUVEC plugs under hypoxic conditions displayed lesser network formation at all time points ($p<0.001$) (Fig. 5N). Taken together these data suggest that purified human myocardial pericytes not only retain mural cell features and support formation of microvascular networks but also exhibit higher angiogenic potential than skeletal muscle pericytes under hypoxia.

### Cardiomyogenic potential of human heart pericytes in vitro

To investigate the cardiomyogenic potential of hHPs, we used DNA demethylation for cardiomyocyte induction *in vitro*, according to published protocols (9). Cultured hHPs were incubated with the induction medium containing 10 μM 5-azacytidine for 72 hours and then in pericyte maintenance medium for 14 additional days. Immunocytochemistry revealed that after cardiomyogenic differentiation, a fraction of hHPs expressed the cardiomyogenic transcription factors Nkx2.5 (Fig. 6A, a) or GATA4 (Fig. 6A, b). However, only a minor fraction of differentiated hHPs expressed unorganized α-sarcomeric actinin (α-actinin) (Fig. 6A, c) or cardiac myosin heavy chain (Fig. 6A, d); no display of mature cardiomyocyte markers cardiac troponin-T (cTn-T) (Fig. 6A, e) or cardiac troponin-I (Fig. 6A, f) was observed, suggesting an immature cardiomyocyte phenotype achieved by chemical induction.

To further examine their cardiomyogenic capacity, GFP+ or CM-Dil-labeled hHPs were co-cultured with rat neonatal cardiomyocytes. Rat cardiomyocytes survived well over the co-culture period with the manifestation of spontaneous yet uncoordinated beating within 48 hours and synchronous contraction of cardiomyocytes over the following 7 days. GFP+ hHPs subsequently added in suspension rapidly settled and adhered to the exposed plastic surface. After co-culturing for 21 days, control cells and co-cultures analyzed by semi-quantitative RT-PCR with human-specific primers showed increases in expression of early cardiac transcription factors Mef2c and GATA4 in co-cultured hHPs (Fig. 6B). Expression of cardiomyocyte protein ANP and cardiac progenitor cell marker c-kit was detectable only

in hHPs after co-culture (Fig. 6B). In contrast, expression of only Mef2c, but not GATA4, ANP, or c-kit, was minimally present in non-co-cultured human adult fat pericytes, with a slight increase in co-cultured counterparts (Fig. 6B), suggestive of negligible cardiomyogenic capacity in this pericyte group. Contraction-like movement was also detected within GFP+ hHPs in 21-day co-cultures when viewed under fluorescence channel (Supplemental Video 5). Nevertheless, close examination using merged fluorescence and phase contrast channels revealed a number of cell fusion/adhesion events between GFP+ hHPs and unlabelled cardiomyocytes (Fig. 6C), making the interpretation of spontaneous contraction and/or cardiomyocyte differentiation difficult (Supplemental Video 6).

To further validate cardiomyocyte phenotypes of differentiated hHPs after co-culturing with rat neonatal cardiomyocytes, we performed immunocytochemistry with cardiac sarcomeric proteins, α-actinin and cTn-T, and fluo-4-based calcium flux imaging respectively. Fluo-4 treatment was applied to monitor changes in cytoplasmic free calcium (Ca), a feature of cells adopting a cardiomyocyte phenotype (32). The results showed that a minor fraction of CM-Dil-labeled, co-cultured hHPs exhibited organized α-actinin (Fig. 6D) and cTn-T (Fig. 6E). Spontaneous calcium oscillations, visible as pulses of green fluorescent light, were detected in a very small fraction of CM-Dil-labeled hHPs using fluo-4 calcium indicator (Fig. 6F). These data suggest committed cardiomyocyte differentiation in, at least, a small proportion of hHPs after co-culture. However, no expression of cTn-I was detected in co-cultured hHPs by immunocytochemistry. These results imply that co-culture with cardiomyocytes induced a more committed cardiomyogenic cell fate in hHPs than chemical induction.

### Cardiomyogenic potential of human heart pericytes in vivo

To corroborate our *in vitro* findings, the cardiomyogenic potential of hHPs was ultimately tested in the cardiac milieu under physiological and ischemic conditions. GFP+ hHPs were injected intramyocardially into acutely infarcted immunodeficient mouse hearts and examined after 1 and 3 weeks (N=3 per time point). Alternatively, GFP+ hHPs were injected into the healthy immunodeficient mouse myocardium for 1 week (N=3). Immunohistochemistry was performed to simultaneously detect GFP and a mature cardiomyocyte marker, cardiac troponin-I (cTn-I). At 1 week post-injection, confocal microscopy revealed the existence of a minor fraction of transplanted hHPs co-expressing GFP and cTn-I within the normal myocardium (Fig. 7A). Similarly, GFP+ hHPs co-expressing cTn-I were detected in the peri-infarct area of the ischemic heart at 1 week post-MI (Fig. 7B). Moreover, a small number of GFP+ hHPs exhibiting integrated sarcomeric patterns was detected by immunofluorescence (Fig. 7C) and immunocytochemistry (Fig. 7D) within the residual myocardium at 3 weeks post-infarction. Further analyses using confocal microscopy unveiled the expression of connexin 43 (Cx43) gap junction protein by a number of GFP/cTn-I dual-positive cells in both normal (Fig. 7E) and ischemic left ventricles (Fig. 7F) at 1 week post-injection. GFP+ CM-like cells co-expressing Cx43 were also detected in the peri-infarct area of the ischemic heart at 3 week post-injection (Fig. 7G), suggestive of conductive functionality in these cells. Altogether these results suggest the cardiomyogenic capacity in a subset of hHPs, not only in ischemic microenvironment but also in the absence of myocardial injury.

## Discussion

Recent progresses in cardiac developmental and stem cell biology as well as encouraging results from clinical trials (SCIPIO and CADUCEUS) using resident cardiac precursor cells have greatly advanced our understanding of native heart stem/progenitor cells (33–37). Despite the increasing knowledge of cardiac regenerative biology, the perivascular cell compartment within the myocardium and its regenerative potential have not yet been fully studied. The importance of pericytes/perivascular cells in contributing to physiological functions, acting as a ubiquitous precursor cell source/niche, and/or participating in pathological conditions has lately been demonstrated by several laboratories (19, 22, 38–42). Additionally, the involvement of perivascular cells in post-injury tissue fibrosis has been suggested in recent studies (43, 44). On the other hand, Chintalgattu et al. lately reported that the substantial depletion of cardiac pericytes, through PDGFR signaling inhibition, consecutive to sunitinib intake leads to coronary microvascular dysfunction, which explains the cause of sunitinib malate-induced cardiotoxicity (26). Above all, pericyte abnormalities in sunitinib-treated mice were observed in hearts but not in skeletal muscles or other organs, indicating cardiac-specific responses to sunitinib toxicity (26). Consequently the pathophysiological role of heart pericytes, the second most frequent cardiac cell type, in cardiac function and regenerative medicine has started to attract attention (45).

Although prior studies by our group and others have extensively characterized microvascular pericytes (CD146+/CD34−/CD45−/CD56−) isolated from multiple human tissues, it remains unclear whether pericytes residing in the heart possess the same perivascular cell phenotypes and/or multi-lineage differentiation capacity (13, 14, 16). Recently, Nees et al. successfully isolated and enriched the pericyte population from hearts of eight mammalian species, including human, using proteolytic perfusion/disintegration and density-gradient centrifugation (46). Enriched heart pericytes can be bulk-cultivated *in vitro* with species-autologous serum and express typical pericyte markers including ALP, 3G5, PDGFRβ, NG2 as well as αSMA and calponin at lower frequencies (46). However, contamination of such enriched pericyte cultures by ECs and other cell types was unavoidable (46). In the current study, we demonstrated that hHPs *in situ* express pericyte markers, including CD146, NG2, PDGFRβ, αSMA and SM-MHC, but not EC markers such as CD31, CD34, CD144, and vWF. Most hHPs also displayed a MSC subset marker, PDGFRα (47), but not desmin, a common pericyte marker (30, 31). Moreover, we did not detect CD117 or Wt1 expression by resident myocardial pericytes, suggesting dissimilarity between hHPs and CD117+ multipotent cardiac precursor cells (CPCs) or Wt1+ epicardial progenitors. No qualitatively significant difference was observed between adult and fetal myocardial pericytes, similar to our previous findings (13). Based on the positive and negative selections of typical pericyte surface antigens with the additional exclusion of CD117, hHPs can be prospectively purified to homogeny by FACS. Sorted hHPs (CD146+/CD34−/CD45−/CD56−/CD117−) can be cultured long term and exhibit very similar phenotypes to their counterparts from other human tissues (13).

The close association of heart pericytes to ECs *in situ* was illustrated by the smallest functional units of bovine coronary microvasculature (consisting of a precapillary arteriole, the capillary net, and postcapillary venules), where not only EC-to-pericyte connections but

also interconnections between most pericytes can be observed (46). The intercellular connections between enriched heart pericytes and ECs were further demonstrated in mixed co-cultures, where dynamic intercellular contacts, connexin43 gap junction formation, and intercellular dye transfer were documented (46). With regard to their microvascular supportive function, our data indicate that sorted hHPs support formation of capillary networks in 2D and 3D Matrigel cultures, with or without ECs, similar to their skeletal muscle counterparts (21). Intriguingly, hHPs upregulate this angiogenic process in 3D Matrigel co-culture under low oxygen conditions, implicating the role of myocardial pericytes in neovascularization following an ischemic insult. Although the mechanism(s) is still unknown, we hypothesize that this phenomenon can be attributed to the increased secretion of angiogenic factors and/or accelerated migration by hHPs in response to the decreased oxygen concentration. Additional studies utilizing purified pericyte populations are needed to reveal the kinetics of pericyte-EC interaction, especially under hypoxic conditions.

Coronary vasculature, including microvessels and capillaries, has been shown to arise from an epicardial origin, which differs from vasculature of other tissues such as skeletal muscle (48–51). In the current study, we demonstrated that hHPs express classic MSC markers *in situ* and in culture and undergo robust mesenchymal differentiations including osteo-, chondro-, and adipogenesis, comparable to pericytes from skeletal muscle and other tissues (13). Despite their seemingly universal mesodermal multipotency and stem/progenitor cell features, it remains unknown whether pericytes of different organs, notably of distinct developmental origins, possess tissue specificity and/or divergent behaviors to pathophysiological conditions (25, 31). Given the capacity to purify pericytes from multiple organs of one subject and by comparing hHPs with hSkMPs isolated from the same donor, we observed differential angiogenic responses to oxygen concentrations and a tissue-specific restriction of skeletal myogenic differentiation in hHPs. These documented cardiac specificities of hHPs are in agreement with the previously reported toxicity of sunitinib specifically in coronary microvascular pericytes (26). We hypothesize that an inhibitory mechanism exists to prevent undesired skeletal myogenesis in the myocardium which may lead to unsynchronized beats and/or catastrophic arrhythmia. Similarly, by comparing genetic profiles of adult mouse cardiac and tail fibroblasts, cardiac fibroblasts have recently been shown to not only display substantial up-regulation of cardiogenic transcription factors but also regulate post-infarction scar formation via Tbx20 activation (52). These data further suggest the organ specificity and unique functions of cardiac stromal cells. Besides, unlike in other human organs, we did not detect *in situ* expression of αSMA by peri-capillary hHPs and desmin by all hHPs. The differential expression pattern of αSMA and desmin in hHPs further implicates the likely differences in contractile function among microvascular mural cells of different tissue origins.

Chong et al. reported a cardiac-resident MSC-like stem cell population in adult mice that can be defined by colony-forming units-fibroblast (CFU-F) potential and capable of broadly differentiating into cell lineages of all three germ layers, including major cardiac cell types: cardiomyocytes, smooth muscle cells, and ECs (9). Further analyses revealed that these cardiac CFU-Fs are derived from the PDGFRα+/Sca-1+/CD31− fraction of adult cardiac

non-myocytes and distinct from CD117+ CPCs (9). Srikanth et al. lately described the isolation of rat fetal cardiac mesenchymal stem cells which not only exhibit morphological and antigenic characteristics of typical BM-derived MSCs but also express multiple embryonic cell markers and differentiate into cell lineages of all three germ layers (53). Furthermore, PDGFRα+ cells residing in the human fetal and adult hearts have recently been identified as a population of multipotent cardiac progenitors with no apparent cardiomyogenic potential (54). Herein we showed that hHPs express PDGFRα natively and in culture and exhibit mesenchymal multipotency except skeletal myogenesis, implicating a developmental connection between hHPs and the reported cardiac mesenchymal precursor populations. Nevertheless, whether other native mesodermal precursor cell subset(s) differing from hHPs constitute human cardiac MSC entity remains to be elucidated. In addition, future studies are needed to investigate if hHPs represent the entire populace of PDGFRα+ and/or CD146+ cardiac MSC/MSC-like progenitors.

Compared with murine multipotent MSC-like cardiac progenitors, the cardiomyogenic potential of human PDGFRα+ cells is diminished (54). Our data from chemical- and co-culture-induced cardiomyogenesis suggest an overall limited cardiomyogenic differentiation capacity in a minor fraction of hHPs *in vitro*, committing mostly to immature cardiomyocytic phenotypes. Nonetheless, a small fraction of hHPs exhibited not only organized α-actinin and cTn-T but also spontaneous calcium oscillations following co-culture induction, implying a more committed cardiomyogenic cell fate acquired by some hHPs. Despite the possibility of cell fusion, results from hHP transplantation *in vivo* suggest the cardiomyogenic potential of hHPs not only in pathological microenvironment but also in healthy myocardium. Furthermore, expression of connexin 43, a key gap junction protein in ventricles, by a number of GFP/cTn-I dual-positive cells further implies their conductive functionality (55). We therefore hypothesize that a minor, yet unidentified subset of hHPs possesses innate cardiomyogenic capacities but requires further activation to attain mature phenotypes. Overall these data indicate a more restricted pattern of adult cardiomyogenesis from stromal precursor cells in the human heart. On the other hand, human fat pericytes did not exhibit cardiomyogenic potential comparable to that of hHPs, indicative of an additional tissue-specific functional discrepancy.

## Conclusion

We herein demonstrate that hHPs can be identified and prospectively purified by classic pericyte markers. hHPs are multipotent mesenchymal precursors residing in the human myocardium with limited cardiomyogenic capacity. Most importantly, these cells not only display an antigenic profile unique to the heart but also exhibit distinct angiogenic responses to hypoxic conditions and tissue specificity in multi-lineage differentiation potential. Collectively, our data imply a pathophysiological role of hHPs beyond that of mere vascular supporting cells. Moreover, this study provides further evidence suggesting evolutionary divergence among pericytes of different origins and establishment of tissue-specific functional and differentiation capacities. Yet the regulatory mechanisms behind their differential cellular functions as well as the therapeutic potential of hHPs in cardiovascular repair/regeneration demand future investigation.

## Supplementary Material

Refer to Web version on PubMed Central for supplementary material.

## Acknowledgments

The authors wish to thank Alison Logar and Megan Blanchard for their expert assistance with flow cytometry, Lindsay Mock for her help with the procurement of human tissues, Dr. Bing Wang for lentiviral-GFP vectors, Dr. Simon Watkins and Center for Biologic Imaging for their assistance in confocal microcopy at the University of Pittsburgh, and Gill Brooker for her assistance with the mouse myocardial infarction model at the University of Edinburgh. This work was supported in part by grants from the Medical Research Council (BP), British Heart Foundation (BP), Commonwealth of Pennsylvania (BP), Children's Hospital of Pittsburgh (BP), National Institute of Health R01AR49684 (JH) and R21HL083057 (BP), William F. and Jean W. Donaldson Endowed Chair at Children's Hospital of Pittsburgh (JH), and Henry J. Mankin Endowed Chair at University of Pittsburgh (JH). CWC was supported in part by an American Heart Association predoctoral fellowship (11PRE7490001). JEB was supported by a British Heart Foundation Centre of Research Excellence doctoral training award (RE/08/001/23904). MC was supported by the California Institute for Regenerative Medicine training grant (TG2-01169).

## References

1. Kumar, V.; Fausto, N.; Abbas, A. Robbins & Cotran Pathologic Basis of Disease, Chapter 12. The Heart. 7. Saunders; Philadelphia, PA: 2004.
2. Bergmann O, et al. Evidence for Cardiomyocyte Renewal in Humans. Science. 2009; 324(5923):98–102. [PubMed: 19342590]
3. Kajstura J, et al. Cardiomyogenesis in the Adult Human Heart. Circulation Research. 2010; 107(2): 305–315. [PubMed: 20522802]
4. Parmacek MS, Epstein JA. Cardiomyocyte Renewal. New England Journal of Medicine. 2009; 361(1):86–88. [PubMed: 19571289]
5. Beltrami AP, et al. Adult Cardiac Stem Cells Are Multipotent and Support Myocardial Regeneration. Cell. 2003; 114(6):763–776. [PubMed: 14505575]
6. Urbanek K, et al. Myocardial regeneration by activation of multipotent cardiac stem cells in ischemic heart failure. Proceedings of the National Academy of Sciences of the United States of America. 2005; 102(24):8692–8697. [PubMed: 15932947]
7. Hansson EM, Lindsay ME, Chien KR. Regeneration Next: Toward Heart Stem Cell Therapeutics. Cell Stem Cell. 2009; 5(4):364–377. [PubMed: 19796617]
8. Laflamme MA, Murry CE. Heart regeneration. Nature. 2011; 473(7347):326–335. [PubMed: 21593865]
9. Chong James JH, et al. Adult Cardiac-Resident MSC-like Stem Cells with a Proepicardial Origin. Cell Stem Cell. 2011; 9(6):527–540. [PubMed: 22136928]
10. Armulik A, Abramsson A, Betsholtz C. Endothelial/Pericyte Interactions. Circ Res. 2005; 97(6): 512–523. [PubMed: 16166562]
11. Gaengel K, Genove G, Armulik A, Betsholtz C. Endothelial-Mural Cell Signaling in Vascular Development and Angiogenesis. Arterioscler Thromb Vasc Biol. 2009; 29(5):630–638. [PubMed: 19164813]
12. Dellavalle A, et al. Pericytes of human skeletal muscle are myogenic precursors distinct from satellite cells. Nat Cell Biol. 2007; 9(3):255–267. [PubMed: 17293855]
13. Crisan M, et al. A Perivascular Origin for Mesenchymal Stem Cells in Multiple Human Organs. Cell Stem Cell. 2008; 3(3):301–313. [PubMed: 18786417]
14. Park TS, et al. Placental Perivascular Cells for Human Muscle Regeneration. Stem Cells and Development. 2011; 20(3):451–463. [PubMed: 20923371]
15. Montemurro T, et al. Differentiation and migration properties of human foetal umbilical cord perivascular cells: potential for lung repair. Journal of Cellular and Molecular Medicine. 2011; 15(4):796–808. [PubMed: 20219017]

16. Chen C-W, et al. Perivascular multi-lineage progenitor cells in human organs: Regenerative units, cytokine sources or both? Cytokine & Growth Factor Reviews. 2009; 20(5–6):429–434. [PubMed: 19926515]
17. Gerlach JC, et al. Perivascular mesenchymal progenitors in human fetal and adult liver. Stem Cells Dev. 2012; 21(18):3258–3269. [PubMed: 22931482]
18. Covas DT, et al. Multipotent mesenchymal stromal cells obtained from diverse human tissues share functional properties and gene-expression profile with CD146+ perivascular cells and fibroblasts. Experimental Hematology. 2008; 36(5):642–654. [PubMed: 18295964]
19. Dellavalle A, et al. Pericytes resident in postnatal skeletal muscle differentiate into muscle fibres and generate satellite cells. Nat Commun. 2011; 2:499. [PubMed: 21988915]
20. Zheng B, et al. Isolation of myogenic stem cells from cultures of cryopreserved human skeletal muscle. Cell Transplant. 2012; 21(6):1087–1093. [PubMed: 22472558]
21. Chen C-W, et al. Human Pericytes for Ischemic Heart Repair. STEM CELLS. 2013; 31(2):305–316. [PubMed: 23165704]
22. Tang W, et al. White Fat Progenitor Cells Reside in the Adipose Vasculature. Science. 2008; 322(5901):583–586. [PubMed: 18801968]
23. Shi S, Gronthos S. Perivascular niche of postnatal mesenchymal stem cells in human bone marrow and dental pulp. J Bone Miner Res. 2003; 18(4):696–704. [PubMed: 12674330]
24. Sacchetti B, et al. Self-Renewing Osteoprogenitors in Bone Marrow Sinusoids Can Organize a Hematopoietic Microenvironment. Cell. 2007; 131(2):324–336. [PubMed: 17956733]
25. Sims DE. Diversity within pericytes. Clin Exp Pharmacol Physiol. 2000; 27(10):842–846. [PubMed: 11022980]
26. Chintalgattu V, et al. Coronary Microvascular Pericytes Are the Cellular Target of Sunitinib Malate–Induced Cardiotoxicity. Science Translational Medicine. 2013; 5(187):187ra169.
27. Zaruba M-M, Soonpaa M, Reuter S, Field LJ. Cardiomyogenic Potential of C-Kit+–Expressing Cells Derived From Neonatal and Adult Mouse Hearts. Circulation. 2010; 121(18):1992–2000. [PubMed: 20421520]
28. Smits AM, et al. Human cardiomyocyte progenitor cells differentiate into functional mature cardiomyocytes: an in vitro model for studying human cardiac physiology and pathophysiology. Nat Protocols. 2009; 4(2):232–243. [PubMed: 19197267]
29. Díaz ME, Eisner DA, O'Neill SC. Depressed Ryanodine Receptor Activity Increases Variability and Duration of the Systolic Ca2+ Transient in Rat Ventricular Myocytes. Circulation Research. 2002; 91(7):585–593. [PubMed: 12364386]
30. Nehls V, Denzer K, Drenckhahn D. Pericyte involvement in capillary sprouting during angiogenesis in situ. (Translated from English). Cell Tissue Res. 1992; 270(3):469–474. (in English). [PubMed: 1283113]
31. Armulik A, Genové G, Betsholtz C. Pericytes: Developmental, Physiological, and Pathological Perspectives, Problems, and Promises. Developmental Cell. 2011; 21(2):193–215. [PubMed: 21839917]
32. Sauer H, et al. Characteristics of calcium sparks in cardiomyocytes derived from embryonic stem cells. Am J Physiol Heart Circ Physiol. 2001; 281(1):H411–H421. [PubMed: 11406510]
33. Chien KR, Domian IJ, Parker KK. Cardiogenesis and the complex biology of regenerative cardiovascular medicine. (Translated from eng) Science. 2008; 322(5907):1494–1497. (in eng).
34. Ptaszek LM, Mansour M, Ruskin JN, Chien KR. Towards regenerative therapy for cardiac disease. The Lancet. 2012; 379(9819):933–942.
35. Chen, WCW.; Péault, B. Encyclopedia of Molecular Cell Biology and Molecular Medicine. Wiley-VCH Verlag GmbH & Co, KGaA; 2013. Development and Renewal of Ventricular Heart Muscle from Intrinsic Progenitor Cells.
36. Bolli R, et al. Cardiac stem cells in patients with ischaemic cardiomyopathy (SCIPIO): initial results of a randomised phase 1 trial. The Lancet. 2011; 378(9806):1847–1857.
37. Makkar RR, et al. Intracoronary cardiosphere-derived cells for heart regeneration after myocardial infarction (CADUCEUS): a prospective, randomised phase 1 trial. The Lancet. 2012; 379(9819):895–904.

38. Armulik A, et al. Pericytes regulate the blood-brain barrier. Nature. 2010; 468(7323):557–561. [PubMed: 20944627]
39. Juchem G, et al. Pericytes in the macrovascular intima: possible physiological and pathogenetic impact. American Journal of Physiology - Heart and Circulatory Physiology. 2010; 298(3):H754–H770. [PubMed: 20023125]
40. Krautler Nike J, et al. Follicular Dendritic Cells Emerge from Ubiquitous Perivascular Precursors. Cell. 2012; 150(1):194–206. [PubMed: 22770220]
41. Tamassia N, et al. Cutting Edge: An Inactive Chromatin Configuration at the IL-10 Locus in Human Neutrophils. The Journal of Immunology. 2013; 190(5):1921–1925. [PubMed: 23355741]
42. Tang Z, et al. Differentiation of multipotent vascular stem cells contributes to vascular diseases. Nat Commun. 2012; 3:875. [PubMed: 22673902]
43. Göritz C, et al. A Pericyte Origin of Spinal Cord Scar Tissue. Science. 2011; 333(6039):238–242. [PubMed: 21737741]
44. Dulauroy S, Di Carlo SE, Langa F, Eberl G, Peduto L. Lineage tracing and genetic ablation of ADAM12+ perivascular cells identify a major source of profibrotic cells during acute tissue injury. Nat Med. 2012; 18(8):1262–1270. [PubMed: 22842476]
45. Nees S, Weiss D, Juchem G. Focus on cardiac pericytes (Translated from English). Pflugers Arch - Eur J Physiol. 2013; 465(6):779–787. (in English). [PubMed: 23443852]
46. Nees S, et al. Isolation, bulk cultivation, and characterization of coronary microvascular pericytes: the second most frequent myocardial cell type in vitro. American Journal of Physiology - Heart and Circulatory Physiology. 2012; 302(1):H69–H84. [PubMed: 22037185]
47. Pinho S, et al. PDGFRα and CD51 mark human Nestin+ sphere-forming mesenchymal stem cells capable of hematopoietic progenitor cell expansion. The Journal of Experimental Medicine. 2013; 210(7):1351–1367. [PubMed: 23776077]
48. del Monte G, et al. Differential Notch Signaling in the Epicardium Is Required for Cardiac Inflow Development and Coronary Vessel Morphogenesis/Novelty and Significance. Circulation Research. 2011; 108(7):824–836. [PubMed: 21311046]
49. Limana F, et al. Identification of Myocardial and Vascular Precursor Cells in Human and Mouse Epicardium. Circ Res. 2007; 101(12):1255–1265. [PubMed: 17947800]
50. Smart N, et al. Thymosin [bgr]4 induces adult epicardial progenitor mobilization and neovascularization. Nature. 2007; 445(7124):177–182. [PubMed: 17108969]
51. Psaltis P, Harbuzariu A, Delacroix S, Holroyd E, Simari R. Resident Vascular Progenitor Cells—Diverse Origins, Phenotype, and Function. (Translated from English). J of Cardiovasc Trans Res. 2011; 4(2):161–176. (in English).
52. Furtado MB, et al. Cardiogenic Genes Expressed in Cardiac Fibroblasts Contribute to Heart Development and Repair. Circulation Research. 2014; 114(9):1422–1434. [PubMed: 24650916]
53. Srikanth GVN, Tripathy NK, Nityanand S. Fetal cardiac mesenchymal stem cells express embryonal markers and exhibit differentiation into cells of all three germ layers. World J Stem Cells. 2013; 5(1):26–33. [PubMed: 23362437]
54. Chong JJH, et al. Progenitor Cells Identified by PDGFR-alpha Expression in the Developing and Diseased Human Heart. Stem Cells Dev. 2013; 22(13):1932–1943. [PubMed: 23391309]
55. Severs NJ, Bruce AF, Dupont E, Rothery S. Remodelling of gap junctions and connexin expression in diseased myocardium. Cardiovascular Research. 2008; 80(1):9–19. [PubMed: 18519446]

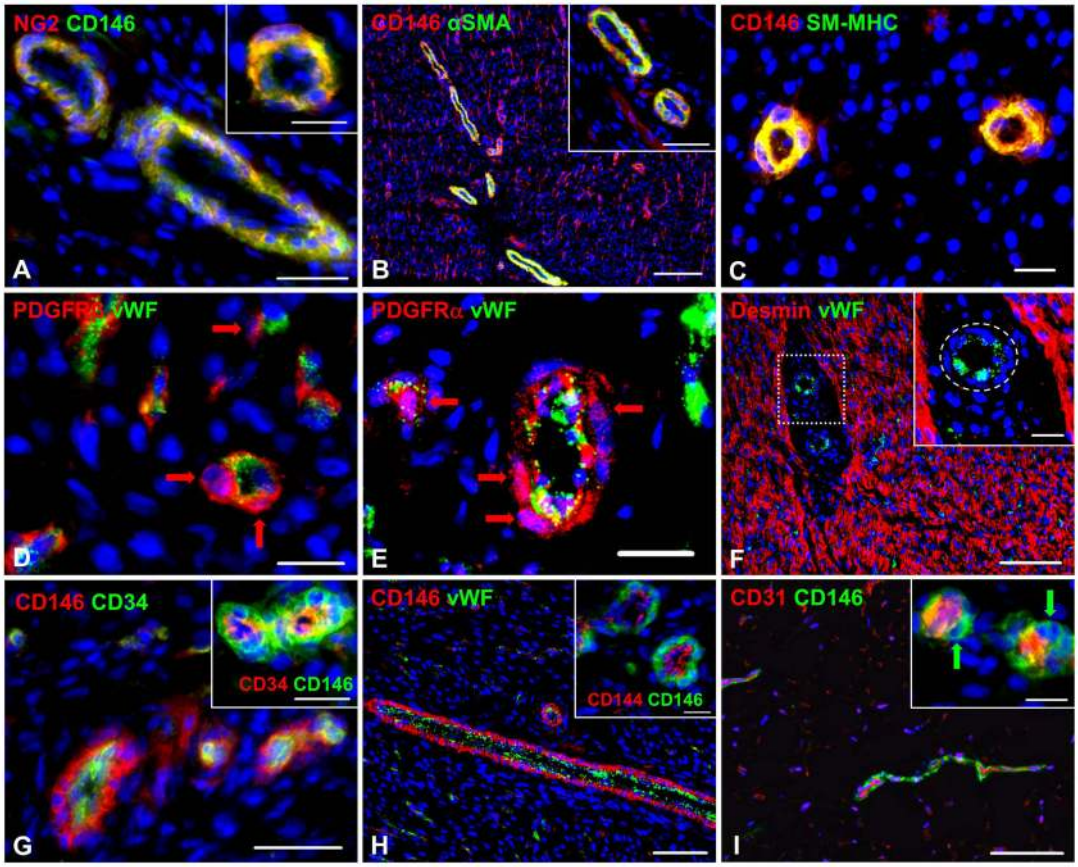


**Figure 1. Identification of resident microvascular pericytes in human ventricular myocardium**

Perivascular cells residing in microvessels of various sizes are identified by co-expression of (A) CD146 (green) and NG2 (red) (scale bar=main, 50μm; inset, 20μm), (B) CD146 (red) and αSMA (green) (scale bar=main, 200μm; inset, 50μm), and (C) CD146 (red) and SM-MHC (green) (scale bar=20μm). Pericytes (red arrows) that are stained positive for (D) PDGFRβ (red) and (E) PDGFRα (red) surround vWF+ endothelial cells (green) (scale bars=20μm). (F) Microvascular pericytes in the myocardium do not express pericyte marker desmin (main, red). Enlargement of a microvessel (inset, dashed circle) within the dotted area further shows no expression of desmin by perivascular cells closely surrounding vWF+ endothelial cells (scale bar=main, 100μm; inset, 20μm). (G) Endothelial cells in microvessels of different sizes are marked by CD34 expression (main, green; inset, red) and tightly enclosed by CD146+ perivascular cells (main, red; inset, green) (scale bars=50μm). (H) A longitudinal section of a microvessel shows that endothelial cells marked by vWF (main, green) are immediately surrounded by perivascular cells expressing CD146 (main, red); a transverse section of microvessels displays that CD146+ pericytes (inset, green) closely surround CD144+ endothelial cells (inset, red) (scale bar=main, 100μm; inset, 20μm) (I) Longitudinal (main) and transverse (inset) sections of microvessels show that CD31+ endothelial cells (red) are tightly encircled by CD146+ perivascular cells (green) (scale bar=main, 50μm; inset, 20μm). Nuclei are stained in blue by DAPI.

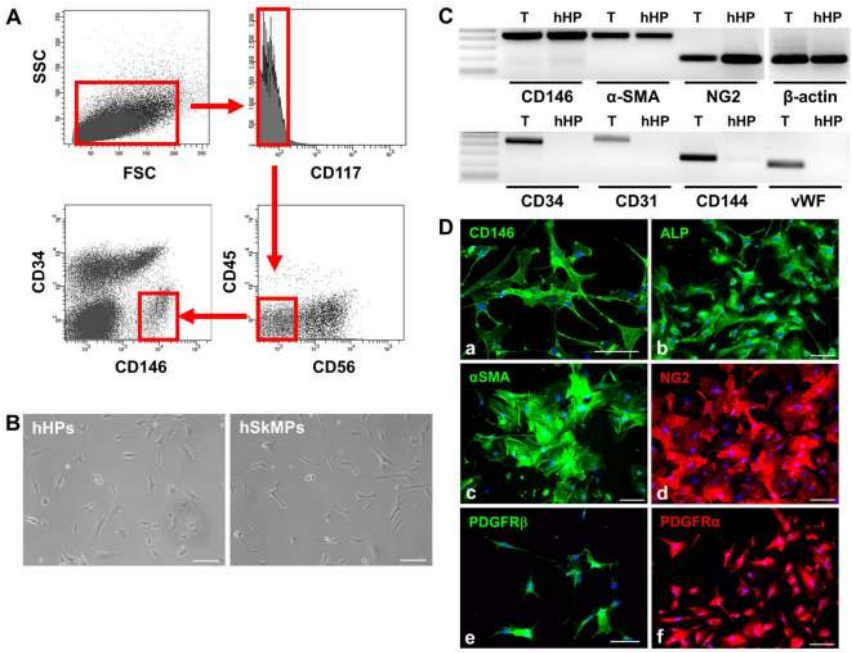


**Figure 2. Purification and culture of human heart pericytes**

(A) FACS sorting of human heart pericytes (hHPs): the CD117− cell fraction was first separated, followed by the selection of CD45−/CD56− cell fraction, and finally separated by CD34−/CD146+ selection. (B) The morphology of cultured hHPs (left panel) was very similar to that of human skeletal muscle pericytes (hSkMPs, right panel) (scale bars=200μm). (C) RT-PCR analysis confirmed that sorted HPs express pericyte markers: CD146, αSMA and NG2, but not endothelial cell markers: CD34, CD31, CD144 and vWF (T: total myocardial lysate, as a positive control). (D) Immunocytochemical analysis revealed that cultured hHPs express typical pericyte markers, including (a) CD146, (b) ALP, (c) αSMA, (d) NG2. (e) PDGFRβ as well as (f) PDGFRα, a multipotent cardiovascular progenitor cell marker (scale bars: (a)(e)=100μm, (b)(c)(d)(f)=200μm).

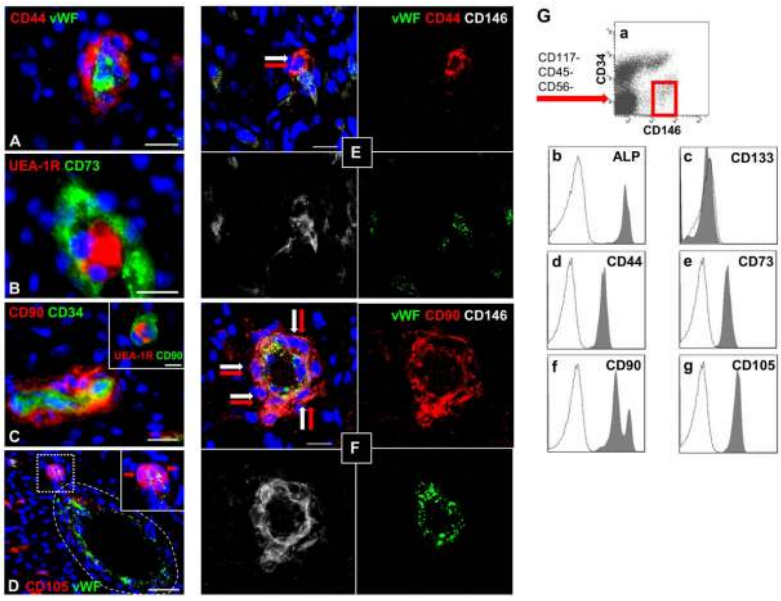


**Figure 3. Human heart pericytes natively express MSC markers**

Left column: Frozen sections of human myocardial tissue were co-stained with antibodies to classic MSC markers, including CD44 (A, red), CD73 (B, green), CD90 ([C] main, red; [C] inset, green), and CD105 (D, red) as well as endothelial cell markers: vWF (A and D, green), the *Ulex europaeus* lectin receptor (UEA-1R) (B and [C] inset, red), or CD34 ([C] main, green). Pericytes surrounding small blood vessels express CD44 (A), CD73 (B), CD90 ([C] main), and CD105 (D) (scale bars: A, B, and [C] main=20μm; D=50μm). Pericytes encircling UEA-1R+ capillaries also express CD90 ([C] inset, scale bar=10μm). Notably, CD105 was only expressed by microvascular pericytes ([D] enlargement, red arrows) but not by perivascular cells surrounding the larger vWF+ vessel (D, dotted encirclement). Middle column: Frozen sections of human myocardial tissue were triple-labeled with antibodies to vWF (green), CD146 (white), and either CD44 (E, red) or CD90 (F, red). Confocal microscopy revealed that pericytes encircling capillaries and microvessels express both CD44 (E) and CD90 (F) in addition to CD146 (white/red arrows) (scale bars=10μm). Right column: (G) hHPs freshly isolated from human myocardium were incubated with antibodies to stem cell and MSC markers and analyzed by flow cytometry. CD146+/CD34−/CD45−/CD56−/CD117− population was first selected (a) before examining for co-expression of ALP (b), CD133 (c), CD44 (d), CD73 (e), CD90 (f), and CD105 (g). Clear histograms (b–g) represent negative control cells stained with non-specific isotype-matched antibodies.

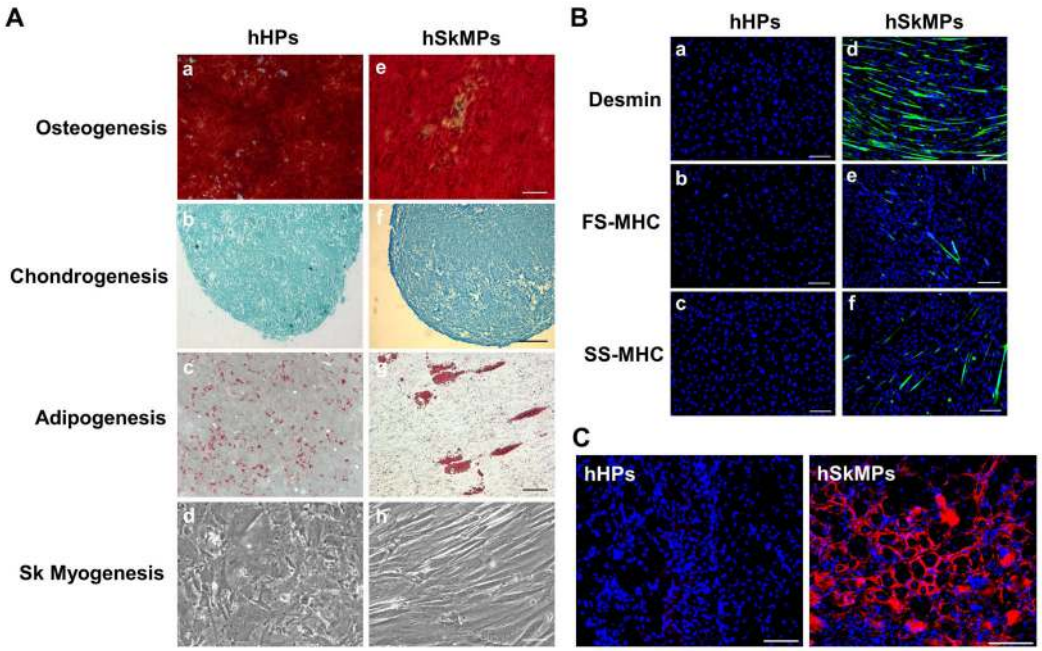


**Figure 4. Human heart pericytes exhibit multi-lineage differentiation potential but, distinctively, no skeletal myogenesis *in vitro* and *in vivo***

(A) Cultured hHPs were examined for mesodermal differentiation capacities in inductive conditions for osteo-, chondro-, adipo-, and skeletal myogenesis respectively. Compared with hSkMPs which exhibited all four mesodermal lineage differentiations (e–h), hHPs displayed robust (a) osteo-, (b) chondro-, and (c) adipogenic differentiations, revealed by alizarin red, Alcian blue, and Oil red O stainings respectively, but (d) did not manifest skeletal myotube formation even after extended incubation for up to 3 weeks (scale bars=100μm). All experiments were independently repeated 3 times. (B) Skeletal myogenesis *in vitro* was further evaluated by immunocytochemistry. Immature and mature myogenic markers, including desmin, fast skeletal myosin heavy chain (FS-MHC), and slow skeletal myosin heavy chain (SS-MHC), were expressed by hSkMPs but not by hHPs after culturing in myogenic (muscle fusion) medium for 7 days (scale bars=200μm). (C) To investigate whether this tissue-specific difference in skeletal myogenesis sustains *in vivo*, fifty thousand cultured hHPs or hSkMPs, isolated from the same donor, were injected into cardiotoxin-injured gastrocnemius muscles of SCID-NOD mice (N=4 per group). Two weeks later, frozen sections of recipient muscles were stained with the human-specific anti-spectrin antibody to reveal newly regenerated myofibers of human origin. In contrast to the large number of human myofibers regenerated by hSkMPs in all specimens, no human spectrin-positive myofiber was detected in hHP-injected muscles (scale bars=100μm).

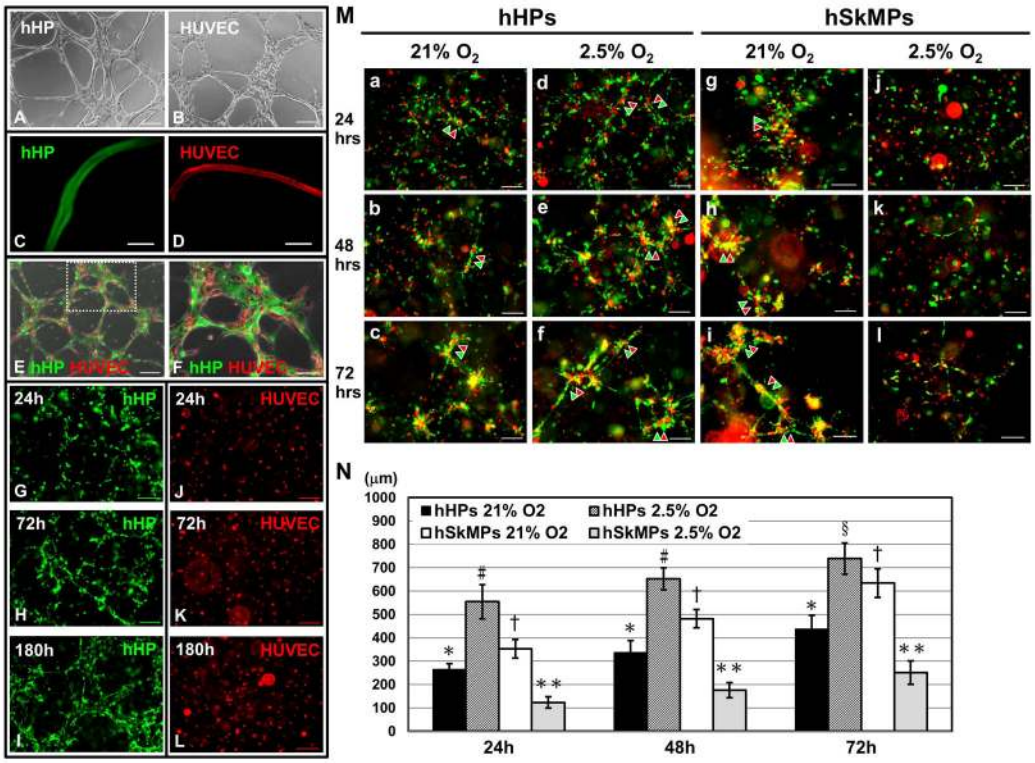


**Figure 5. Microvascular supportive function of human heart pericytes**

(A) Human heart pericytes (hHPs) seeded into Matrigel-coated wells formed network structures within 6–12 hours, similar to (B) typical capillary-like networks formed by human umbilical cord vein endothelial cells (HUVECs) during the same time frame. (C) Confocal microscopy unveiled formation of tubal structures by dye-labeled hHPs (green) in Matrigel-coated culture at 72 hours, comparable to (D) endothelial tubes formed by dye-labeled HUVECs (red) at the same time. (E) Dye-labeled hHPs (green) and HUVECs (red) co-formed network structures within 6–12 hours on Matrigel-coated surfaces. (F) Enlargement of the dotted area in (E) showed that HUVECs appear to morphologically align with hHPs. (G–I) To simulate native capillary formation, hHPs were evenly encapsulated into 3D Matrigel plugs for up to 180 hours. hHPs formed 3D network structures with structural reorganization and maturation over time. (J–L) HUVECs encapsulated into 3D Matrigel plugs in the same manner were unable to form any organized structure. (All scale bars=200μm, except (C–D) scale bars=50μm and (F) scale bar=100μm) (M) When dye-labeled human heart pericytes (hHPs, green) and HUVECs (red) were evenly casted into a 3D Matrigel plug (a–c) under the ambient oxygen concentration (21% $O_2$) *in vitro*, these two types of cells migrated and together formed network structures within 72 hours, with progressive collocations of hHPs and HUVECs. (d–f) When Matrigel plugs were exposed to hypoxic culture conditions (2.5% $O_2$), the co-formation of network structures was facilitated over time. (g–i) In comparison, human skeletal muscle pericytes (hSkMPs) co-formed similar network structures with HUVECs under 21% $O_2$ but (j–l) showed notably diminished sprouting responses and network formation under hypoxic conditions. Representative network structures at each time point were indicated by green and red arrow heads. (all scale bars=200μm) (N) Quantification of network cord length (N=3 plugs per

group) disclosed that the network formation by hHPs and HUVECs was significantly facilitated under hypoxic culture conditions at all time points. On the contrary, networks formed by hSkMPs and HUVECs were significantly reduced under the same hypoxic condition. (At each time point: *$p$<0.001, versus hSkMPs 2.5% $O_2$; $^{\#}p$<0.001, versus all groups; $^{\S}p \leq 0.005$, versus all groups; $^{\dagger}p \leq 0.001$, versus hHPs 21% $O_2$ and hSkMPs 2.5% $O_2$; **$p$<0.001, versus all groups; all data presented as mean ± SD)

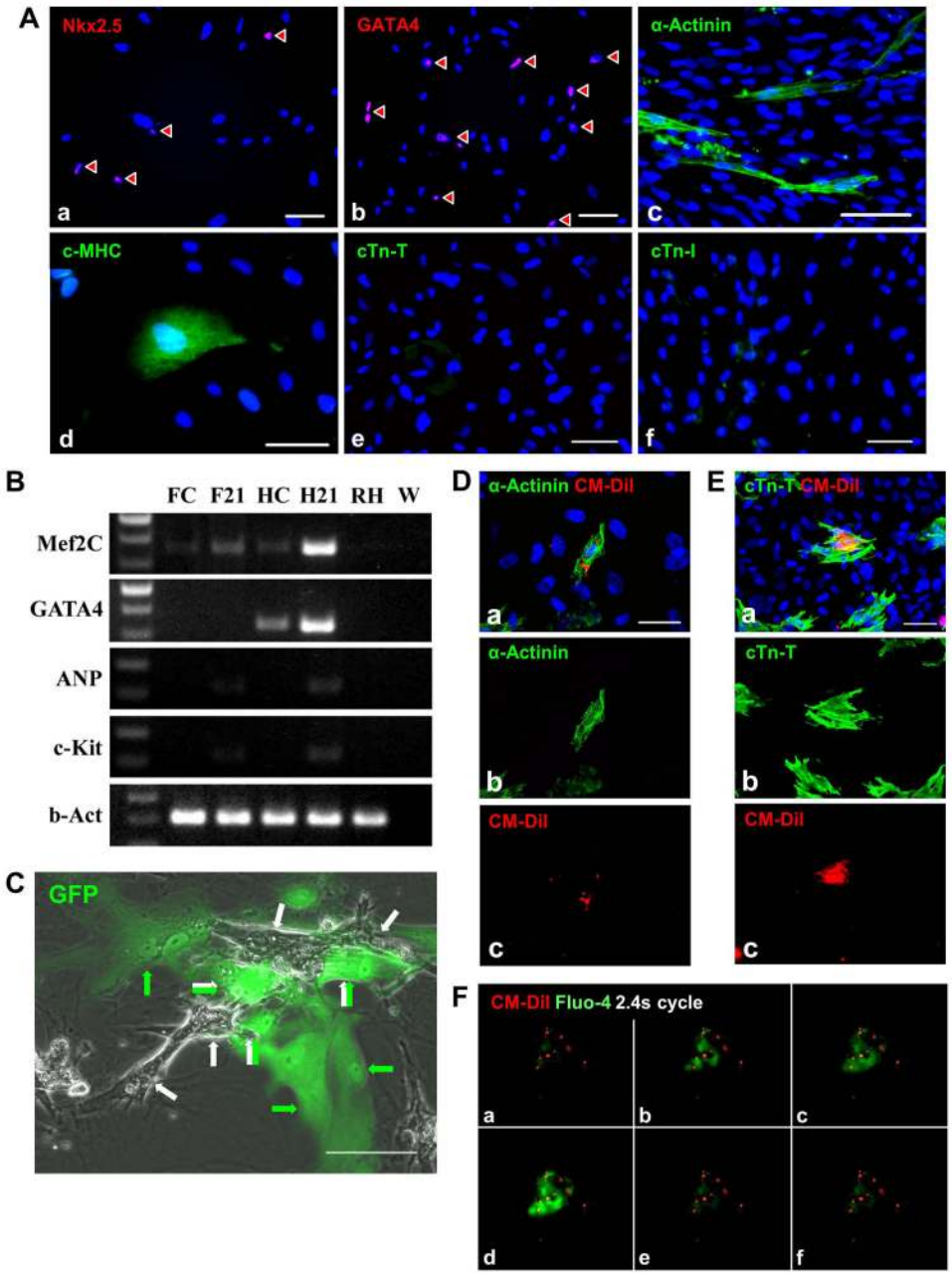


**Figure 6. Cardiomyocyte differentiation of human heart pericytes *in vitro***

(A) After incubation in cardiomyogenic induction medium containing 10 μM 5-azacytidine for 72 hours and then in pericyte maintenance medium for additional 14 days, a fraction of hHPs expressed (a) Nkx2.5 and (b) GATA4. A minor fraction of hHPs also expressed unorganized (c) α-actinin and (d) cardiac myosin heavy chain (c-MHC), but not (e) cardiac troponin-T (cTn-T) or (f) cardiac troponin-I (cTn-I) (all scale bars=100μm). Cardiomyogenic capacity of hHPs was further investigated *in vitro* by co-culturing GFP+ hHPs with rat neonatal cardiomyocytes (rNCMs). (B) Gene expression of cardiomyocyte-associated markers in human pericytes after co-culture for 21 days. Non-co-cultured cells maintained in the same culture conditions served as controls. The specificity of human

primers was confirmed by negative signals of rat neonatal heart lysate. Water was used as blank control (FC: human fat pericyte control; F21: human fat pericytes after co-culture; HC: human heart pericyte control; H21: human heart pericytes after co-culture; RH: rat neonatal heart lysate; W: water). (C) A representative merged image from phase contrast and fluorescence time-lapse series taken after 21 days of co-culture showed a number of cell fusion/adhesion events (green/white arrows) between GFP+ hHPs (green arrows) and unlabelled rNCMs (white arrows) (scale bar=100μm). The full time-lapse movie is listed as Supplemental Video 6. After co-culturing with rNCMs, a minor fraction of CM-Dil-labeled hHPs exhibited (D) organized α-actinin (scale bar=50μm) and (E) cTn-T (scale bar=100μm). Fluo-4-based calcium imaging was further used to detect spontaneous cytoplasmic calcium flux in co-cultured hHPs. (F) A representative montage image from a cycle of 2.4 seconds illustrated progressive rise and fall of cytoplasmic calcium (represented by the change in green fluo-4 fluorescence intensity) within a single CM-Dil stained hHP (red punctate) (a–f, chronologically arranged, interval=0.4 second).

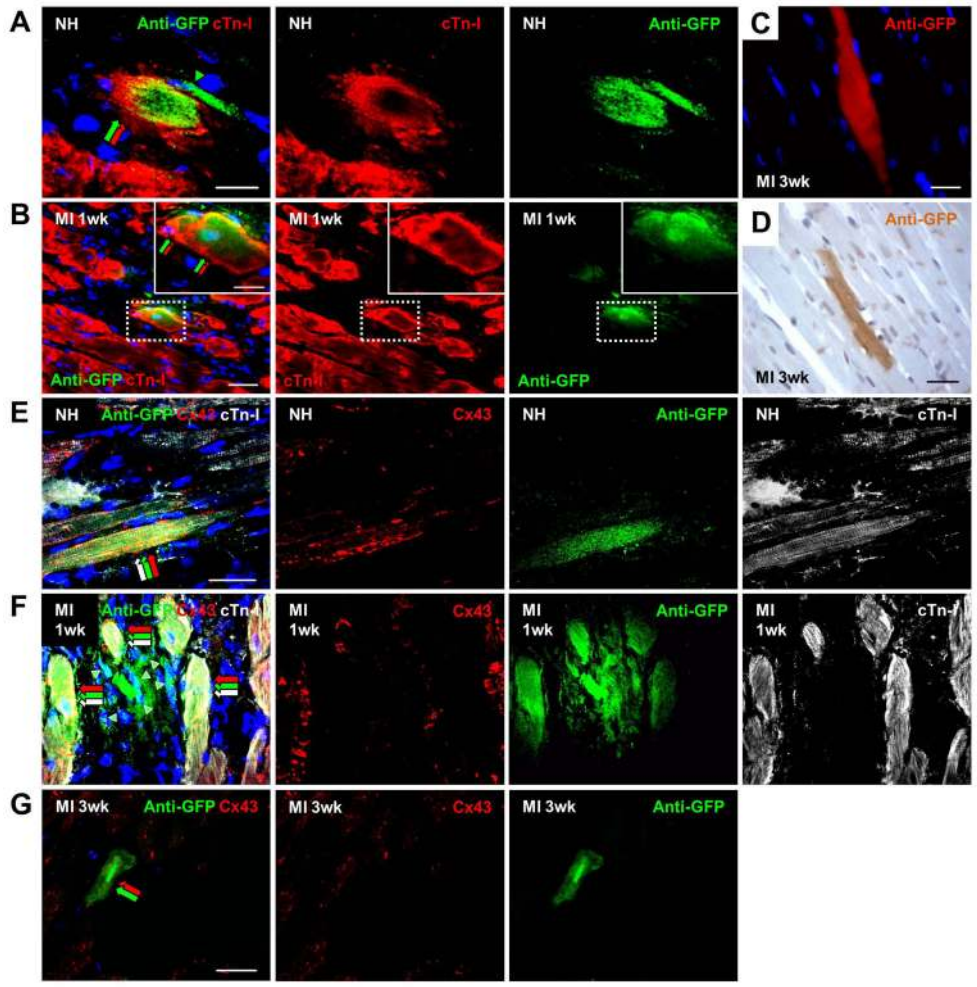


**Figure 7. Cardiomyocyte differentiation of human heart pericytes *in vivo***

The cardiomyogenic potential of hHPs was ultimately tested *in vivo* by transplanting $3\times10^5$ GFP+ hHPs into normal healthy hearts for 1 week (N=3) or acutely infarcted hearts for 1 and 3 weeks (N=3 per time point) in immunodeficient mice. (A) At 1 week post-infarction, confocal microscopy revealed GFP+ hHPs co-expressing a mature cardiomyocyte marker, cardiac troponin-I (cTn-I), in healthy hearts (green/red arrows), with additional GFP+ cells (green arrow head) in the surrounding (cTn-I in red, anti-GFP in green) (scale bar=10μm). (B) Similarly, a minor fraction of GFP+ hHPs co-expressing cTn-I was present in the peri-infarct area of infarcted hearts (green/red arrows, dotted area enlarged in [B] inset) while additional GFP+ cells (green arrow heads) remained in the surrounding interstitium (scale bar=main, 20μm; inset, 10μm). At 3 weeks post-infarction, a small number of GFP+ hHPs exhibiting integrated sarcomeric patterns within the residual myocardium were detected by (C) immunofluorescence and (D) chromagen-based immunocytochemistry (scale bars: (C)=10μm, (D)=25μm). These results suggest the cardiomyogenic capacity of hHPs not only in ischemic microenvironment but also in the absence of myocardial injury. Further confocal microscopic studies showed that at 1 week post-injection, the expression of connexin 43 (Cx43) gap junction protein by a number of GFP/cTn-I dual-positive cells (red/green/white arrows) in both (E) normal and (F) ischemic myocardium (Cx43 in red, anti-GFP in green,

cTn-I in white) (scale bars: (E)=20μm, (F)=10μm). Note that more GFP+ donor cells (green arrow heads) were scattered in the surrounding interstitium. (G) GFP+ CM-like cells expressing Cx43 (green/red arrows) were also detected in ischemic hearts at 3 weeks post-infarction (Cx43 in red, anti-GFP in green) (scale bar=20μm), suggestive of conductive functionality in these cells.